Journal of Biomolecular NMR, **15:** 295–307, 1999.
KLUWER/ESCOM

Direct determination of the heteronuclear T_1/T_2 ratio by off-resonance steady-state magnetization measurement: Investigation of the possible application to fast exchange characterization of ^{15}N-labeled proteins

Marc Guenneugues[a,*], Patrick Berthault[b], Hervé Desvaux[b,**] & Maurice Goldman[c]
[a]*Département d'Ingénierie et d'Etude des Protéines,* [b]*Service de Chimie Moléculaire and* [c]*Service de Physique de l'Etat Condensé, Laboratoire Commun de R.M.N. CEA/Saclay, F-91191 Gif sur Yvette cedex, France*

Received 6 August 1999; Accepted 13 October 1999

Key words: fast exchange, heteronuclear relaxation, off-resonance rf irradiation, protein dynamics, steady-state magnetization, T_1/T_2 ratio

Abstract

The ^{15}N steady-state magnetization in the presence of off-resonance rf irradiation is an analytical function of the T_1/T_2 ratio and of the angle between the ^{15}N effective field axis and the static magnetic field direction. This relation holds whatever the relaxation mechanisms due to motions on the nanosecond time scale, and the size of the spin system. If motions on the micro- to millisecond time scale are present (fast exchange), the same observable depends also on their spectral density at the frequency of the effective field. The cross-peak intensity in each 2D ^{15}N-^{1}H correlation map is directly related to the dynamic parameters, so that the characterization of fast exchange phenomena by this method is in principle less time-consuming than the separate measurement of self-relaxation rates. The theory of this approach is described. Its practical validity is experimentally evaluated on a ^{15}N-labeled 61 amino acid neurotoxin. It turns out that existing equipments lead to non-negligible biases. Their consequences for the accuracy attainable, at present, by this method are investigated in detail.

Introduction

The study of the dynamics of the protein backbone through heteronuclear relaxation experiments (Kay et al., 1989; Wagner, 1993; Palmer et al., 1996) follows a new trend consisting in the identification of concerted motions. The exploration of the pico- to nanosecond motions of secondary structure elements can be based on statistical analysis of the heteronuclear longitudinal to transverse self relaxation time ratios (T_1/T_2) (Brüschweiler et al., 1995; Tjandra et al., 1995; 1996a,b) while the characterization of slower motions in the 10 μs – 100 ms range requires dedicated experiments based on off-resonance self-relaxation rate measurements (Akke et al., 1998). Both approaches encounter their own experimental limitations, which explain the search for using supplementary measurements as the CSA/dipolar cross-correlation (Fushman et al., 1998, Kroenke et al., 1998) or the residual dipolar coupling (de Alba et al., 1999). Indeed, the statistical exploitation of T_1/T_2 ratios requires high accuracy in their determination to avoid dealing with pseudo-energy landscapes that are too smooth and turn to inhibit the determination of the minima (Lee et al., 1997). On the other hand, although various methods have been proposed to determine exchange correlation times (Szyperski et al., 1993; Orekhov et al., 1994; Akke and Palmer, 1996; Zinn-Justin et al., 1997), the precision in their determination is not sufficient to base on their relative values, the assignment of which amide nitrogens experience the same concerted motions. Mapping the fast exchange spectral density function is indeed very time consuming, since each point is extracted out of 5 to 10

*Present address: Bijvoet Center for Biomolecular Research, Utrecht University, Padualaan 8, 3584 CH Utrecht, The Netherlands.
**To whom correspondence should be addressed. E-mail: hdesvaux@Cea.fr

2D maps. The use of the accordion technique reduces the experiment duration (Mandel and Palmer, 1994; Guenneugues et al., 1999b) but at the cost of a lower precision.

We report herein the exploration of a new procedure based on the measurement of the ^{15}N steady-state magnetization in the presence of an off-resonance rf irradiation. Cross-relaxation with other coherences, in particular involving the proton bath, is suppressed by irradiating the protons. Each cross-peak volume in the derived 2D ^{15}N-^{1}H correlation maps is directly related to the T_1/T_2 ratio of the corresponding ^{15}N nucleus. We show below that in the general case this dependence is described by an analytical function. Variation of two tunable parameters, amplitude ω_1^S and offset Δ_S of the ^{15}N irradiation, should enable the determination of both the T_1/T_2 ratio and the possible contribution of fast exchange processes. The analytical nature of the general theoretical solution makes it possible to detect experimental biases, and some of them, such as the rf field inhomogeneity, can explicitly be taken into account.

Theory

Among the explored methods based on the measurement of steady-state magnetization in the presence of off-resonance rf irradiation (see Desvaux and Berthault (1999) for a review), nobody considered, to our knowledge, the system of a heteronucleus, a proton bath and all relaxation contributions resulting from dipolar (DD) and chemical shift anisotropy (CSA) interactions, from external sources and from fast exchange. This case is treated below.

We first consider the simplest case, that of an isolated *I*–*S* spin pair relaxing by mutual dipolar interaction, where *I* is a proton directly bound to a heteronucleus *S*. The spin *S* is taken to be ^{15}N but it can be ^{13}C or ^{31}P as well. The rf irradiation of amplitude ω_1^S applied at an offset Δ_S from the ^{15}N resonance frequency (respectively ω_1^I and Δ_I for the proton) defines in the rotating frame an effective field axis for the *S* spin (respectively for *I*) which makes an angle $\theta_S = \arctan(\omega_1^S/\Delta_S)$ (respectively $\theta_I = \arctan(\omega_1^I/\Delta_I)$) with the static magnetic field direction. The theory of relaxation applied to nitrogen magnetization $\langle S_Z\rangle$ aligned with the effective field *OZ* in the rotating frame is very similar to that of the homonuclear case (Desvaux and Goldman, 1992) except that the transverse cross-relaxation between two different species is absent. One then finds:

$$\frac{d}{dt}\langle S_Z\rangle = -\frac{1}{T_{1\rho}^{\text{off}}}\langle S_Z\rangle - \cos\theta_I\cos\theta_S\sigma_{IS}\langle I_Z\rangle + \frac{1}{T_1}\cos\theta_S S_0 + \cos\theta_S\sigma_{IS}I_0 \qquad (1)$$

where S_0 and I_0 are the thermal equilibrium magnetizations of the nitrogen and the proton, respectively. σ_{IS} is the heteronuclear dipolar cross-relaxation rate and $T_{1\rho}^{\text{off}}$ is the nitrogen off-resonance relaxation time, equal to (Goldman, 1999):

$$\frac{1}{T_{1\rho}^{\text{off}}} = \frac{1}{T_1}\cos^2\theta_S + \frac{1}{T_2}\sin^2\theta_S \qquad (2)$$

When the proton irradiation is applied on-resonance ($\theta_I = 90°$), the proton steady-state magnetization $\langle I_Z^{eq}\rangle$ is negligible according to the difference of amplitude between the static and rf fields. From Equation 1, one obtains the nitrogen steady-state magnetization:

$$\langle S_Z^{\text{eq}}\rangle = \frac{\cos\theta_S(S_0 + I_0\sigma_{IS}T_1)}{\cos^2\theta_S + \sin^2\theta_S(T_1/T_2)} \qquad (3)$$

The ratio of the longitudinal to transverse self-relaxation times T_1/T_2 can therefore be obtained from the variation of the steady-state magnetization of the heteronucleus as a function of the angle θ_S.

The extension of this result to the real case can be performed as follows. In a first step, we consider a system composed of one spin *S* and *n* protons I^k. The mutual dipolar interactions between these spins and the CSA of the nitrogen are the interactions which contribute to relaxation. Taking into account the possible cross-correlation cross-relaxation processes between all these interactions, the equation of evolution of the nitrogen magnetization is:

$$\begin{aligned}\frac{d}{dt}\langle S_Z\rangle = &-\frac{1}{T_{1\rho}^{\text{off}}}\langle S_Z\rangle + \frac{1}{T_1}\cos\theta_S S_0 \\ &- \cos\theta_S\left(\sum_k \cos\theta_I\sigma_{I^kS}\langle I_Z^k\rangle - \sigma_{I^kS}I_0\right) \\ &- \sum_k \delta_{S,I^kS}^{\theta^I,\theta^S}\langle 2I_Z^k S_Z\rangle \\ &- \sum_{k\neq l}\delta_{S,I^kSI^l}^{\theta^I,\theta^S}\langle 4I^kI^lS_Z\rangle \end{aligned} \qquad (4)$$

The successive terms on the right-hand side are the self-relaxation of $\langle S_Z\rangle$, the cross-relaxation resulting

from the I^k–S dipolar interaction, the cross-relaxation resulting from the cross-correlation between the CSA of S and the dipolar interaction between I^k and S, and finally the cross-relaxation resulting from cross-correlation between I^k–S and I^l–S dipolar interactions. The notations are from Desvaux and Berthault (1999), where the expressions of these different rates are given as a function of the spectral densities. The off-resonance self-relaxation rate $1/T_{1\rho}^{\text{off}}$ is still related to the longitudinal and transverse self-relaxation rates by Equation 2, but the latter rates are now obtained by summing all contributions resulting from dipolar and CSA interactions.

The dipolar cross-relaxation rates (terms proportional to I_Z^k) still vanish when $\theta_I = 90°$, as well as the cross-relaxation rate between S_Z and $2I_Z^k S_Z$ (Zinn-Justin et al., 1997; Felli et al., 1998). Finally, the cross-relaxation resulting from cross-correlation between two dipolar interactions involving twice the heteronucieus (S–I^k and S–I^l) depends only on the spectral density value at the proton frequency when $\theta_I = 90°$ (Desvaux and Berthault, 1999). In the slow tumbling regime ($\omega_I \tau_c \gg 1$), valid for proteins, this cross-relaxation mechanism is inefficient. Moreover, this term is reduced by the fact that the second proton is at a greater distance from the nitrogen nucleus than is the amide proton. As a consequence, for $\theta_I = 90°$ all cross-relaxation mechanisms between S_Z and other coherences almost vanish and the steady-state magnetization of the nitrogen keeps the form of Equation 3:

$$\langle S_Z^{\text{eq}} \rangle = \frac{A \cos\theta_S}{\cos^2\theta_S + \sin^2\theta_S (T_1/T_2)} \tag{5}$$

where:

$$A = S_0 + \sum_k \sigma_{I^k S} T_1 I_0 \tag{6}$$

It can be shown that Equation 2 remains valid for other relaxation mechanisms (Goldman, 1999) provided that the correlation time is such that $\Omega_S \tau_c \ll 1$, where the effective field amplitude $\Omega_S = \sqrt{\Delta_{S^2} + (\omega_1^S)^2}$ is at most equal to 250 kHz for classical experimental equipment. Consequently, Equation 5 is also valid if any external random field or paramagnetic contribution to self-relaxation of the heteronucleus is considered.

In the case of fast exchange contributions to relaxation, the corresponding correlation time τ_e, may be comparable to or larger than $1/\Omega_S$. Equation 4 is still valid but Equation 2 has to be modified to make explicit the dependence of the rate $1/T_{1\rho}^{\text{off}}$ on the exchange spectral density $J_{\text{ex}}(\Omega_S)$ at the effective field amplitude Ω_S (Davis et al., 1994; Desvaux et al., 1995b; Akke and Palmer, 1996; Zinn-Justin et al., 1997):

$$\frac{1}{T_{1\rho}^{\text{off}}} = \frac{1}{T_1}\cos^2\theta_S + \frac{1}{T_2}\sin^2\theta_S + \sin^2\theta_S J_{\text{ex}}(\Omega_S) \tag{7}$$

Then the nitrogen steady-state magnetization is:

$$\langle S_Z^{\text{eq}} \rangle = \frac{A \cos\theta_S}{\cos^2\theta_S + \sin^2\theta_S (T_1/T_2) + \sin^2\theta_S T_1 J_{\text{ex}}(\Omega_S)} \tag{8}$$

In the following we assume a two-site jump model for the exchange with respective populations p_a and p_b, and a resonance frequency splitting $\delta\nu$. The function J_{ex} is equal to (Deverell et al., 1970; Brüschweiler and Ernst, 1992):

$$J_{\text{ex}}(\Omega) = 4\pi^2 p_a p_b \delta\nu^2 \frac{\tau_{\text{e}}}{1 + \Omega^2 \tau_{\text{e}}^2} \tag{9}$$

Assuming that the SI^k, SI^l dipole–dipole cross-correlation cross-relaxation can safely be neglected, Equation 8 is general whatever the relaxation mechanism and the size of the proton spin system. Any deviation from Equation 8 should result from experimental biases.

According to Equation 8, the steady-state magnetization of the nitrogen at an angle θ_S and rf field amplitude ω_1^S is directly related to the dynamics on the nanosecond time scale through T_1/T_2 and on the microsecond to millisecond time scale through $J_{\text{ex}}(\Omega_S)$. Varying Δ_S and ω_1^S gives access not only to the T_1/T_2 ratio, but also to the parameters of the exchange, the exchange correlation time τ_e and $p_a p_b \delta\nu^2 T_1$. The two parameters can separately be determined since, for instance, at constant angle θ_S, $\langle S_Z^{\text{eq}} \rangle$ is still dependent on Ω through the exchange correlation time τ_e, in a manner similar to what has been proposed for protons (Desvaux et al., 1995b). A careful investigation of this approach is thus necessary for two main applications:

1. If the accessible range of Ω_S is such that $\Omega_S \tau_e \sim 1$, the variation of $\langle S_Z^{\text{eq}} \rangle$ as a function of θ_S and ω_1^S yields T_1/T_2 and the parameters of the exchange. The determination of the exchange correlation time would help to search for coherent slow deformation involving different amino acids.
2. When $\Omega_S \tau_e \gg 1$ or when no exchange contribution is present, the non-linear fitting of the experimental data to Equation 5 gives access to

T_1/T_2. Finally, in the last case ($\Omega_S \tau_e \ll 1$) a non-negligible contribution from exchange affects the determination of T_1/T_2. This contribution is likely to be small, since the effective field amplitude Ω_S is usually much larger than in any on-resonance self-relaxation rate experiment. In most cases, we expect to determine the T_1/T_2 ratios with a very restricted contribution from chemical exchange. They can then safely be used for studies of possible anisotropic Brownian motions of the protein.

Materials and methods

Experiments were carried out at 310 K on a 5 mM ^{15}N labeled sample of toxin α (Drevet et al., 1997) dissolved in H_2O:D_2O 90:10. The spectra were acquired on Bruker DRX 500 and 600 spectrometers with 5-mm ^{1}H/^{13}C/^{15}N and broadband inverse probeheads equipped with pulsed field gradients. The ^{15}N rf field strength and distribution were measured using sequences derived from that published by Guenneugues et al. (1999a). The ^{15}N steady-state magnetization was measured after an INEPT transfer, in order to benefit from the greater sensitivity of the proton nucleus. Measurement as a ^{1}H-^{15}N 2D-correlation map was normally used to avoid peak overlap (see Section 'Pulse sequence' and Figure 2). The 2D maps were composed of 256 FIDs of 1532 points each, acquired in States-TPPI mode. For each FID, the number of accumulations was 24. The interscan delay was lengthened in the course of the development of the experiment to avoid electronic instabilities, bringing the acquisition of a 2D map from 4 h to 5 h. The spectral width in the F1 dimension was 29.6 ppm and in the F2 dimension 6.40 ppm, centered on the amide resonances. At each rf field amplitude, the spectra corresponding to the different angles θ_S were acquired in an interleaved way, in order to minimize the effect of the spectrometer frequency drift during the complete acquisition (Tjandra et al., 1995). The point at $\theta_S = 0°$, which required the use of a slightly different sequence (see below) was recorded separately. The offsets Δ_S were chosen positive and negative with respect to the carrier frequency so as to insure a larger sampling of θ_S values even for ^{15}N spins which resonate at the edge of the spectrum. Although it is desirable to minimize temperature fluctuations of the sample resulting from the use of different rf field strengths by applying dummy rf irradiation during the interscan delay (Wang and Bax, 1993), the amplifier limitations made this impossible.

All spectra were processed using Felix95 software (Biosym/MSI, 1995). The matrices were apodized in both dimensions by a shifted sinebell function before Fourier transformation. The processed spectra contained 256 and 1024 points in both dimensions, respectively. Automatic baselines correction was applied using a Flatt algorithm in the acquisition dimension. The cross-peak integrals were fitted against Equations 5 and 8 using home-written software based on the Levenberg-Marquardt algorithm (Press et al., 1992). The resonance offset of each ^{15}N amino-acid was explicitly taken into account. The uncertainties on the integrals were estimated as 3.5% of the average A values, and were taken to be constant for all measurements. With this figure for the uncertainty, the average value of the reduced χ^2 between the best-fit theoretical curves (Equation 5) and the experimental data is compatible with 1, proving reasonable estimation of the experimental uncertainties. The uncertainties on the fitted parameters were evaluated by a Monte-Carlo simulation. Synthetic data sets are generated by adding to each measured intensity a random value on a Gaussian distribution of standard deviation defined by the uncertainty on this points. These synthetic data sets are fitted by the same Marquardt algorithm as above. This procedure was repeated 500 times for each amino acid, and the average and standard deviation of T_1/T_2 were computed. Since biases are present in the measurements presented in Figures 3 and 4, the confidence on the extracted T_1/T_2 values and their standard deviation is necessarily low.

For the numerical simulations, the program first computed the self- and cross-relaxation rates for all angles θ_I and θ_S. Then the relaxation matrix was inverted by LU decomposition (Press et al., 1992) and the steady-state values of all the considered coherences were computed. This procedure was repeated for different offsets Δ_S and different rf field strengths ω_1^S. The resulting sets of data were fitted against Equations 5 and 8 using the software described above.

Results

Numerical simulations

In practice, it is impossible to spin-lock simultaneously all protons at $\theta_I = 90°$. Thus a coupling exists between the nitrogen and proton spins bath through dipolar and CSA/dipole cross-relaxation. Earlier stud-

ies of the proton steady-state magnetization in the presence of off-resonance rf irradiation showed that, when one considers large molecules ($\omega_I \tau_c \gg 1$), the equilibrium proton magnetization is small for large angles θ_I (Desvaux and Goldman, 1992). Therefore maximizing the angle θ_I has two favorable effects, which allow one to neglect the influence of the proton magnetization on that of nitrogen: firstly, the interaction between the two spin baths is decreased and secondly, the steady-state magnetization of the proton spin ($\langle I_Z^{k^{eq}} \rangle$) is minimized.

This feature has been assessed by numerical simulations. The procedure consists in determining the ^{15}N steady-state magnetization from the expression of the relaxation matrix at various angles θ_I and θ_S, and in determining the T_1/T_2 ratio by fitting the variation of $\langle S_Z^{eq} \rangle$ as a function of θ_S to Equation 5 at constant angle θ_I. The relaxation rates were computed as described in Felli et al. (1998) assuming a rigid isotropic Brownian motion (correlation time of 4 ns, static magnetic field of 11.7 T (Guenneugues et al., 1997)), and considering contributions to relaxation from CSA on the nitrogen and all dipole–dipole interactions. The NMR solution structure of toxin α (Zinn-Justin et al., 1992) was used to define the spin geometry. For each nitrogen, a cutoff of 6 Å was used in order to simulate the influence of the complete proton bath. The steady-state values of about 60 coherences of the types $\langle S_Z^{eq} \rangle$ or $\langle I_Z^{k^{eq}} \rangle$ or $\langle 2 S_Z I_Z^{k^{eq}} \rangle$ were computed. It results from this study that the relative difference between the exact and fitted T_1/T_2 values reaches 10% for $\theta_I = 0°$ (the best-fit value being always smaller) but is below 1.5% for θ_I larger than 70° (Table 1).

A fast exchange contribution was then introduced so that the dependence of the steady-state values on θ_S and Ω_S was described by Equation 8, which differs from Equation 5 by a term explicitly depending on Ω_S. However, using only one rf field strength ω_1^S is not sufficient to accurately determine the exchange spectral density function in view of the magnitude of the experimental uncertainties. Indeed, as shown in Figure 1, the introduction of chemical exchange does not significantly change the curve, so that the discrimination between the behavior expected from Equation 5 and Equation 8 is not easy. However, a reasonable determination of the exchange correlation time τ_e, can be obtained using various rf field amplitudes ω_1^S (Figure 1), since it acts on the curvature. On the other hand, the parameter $T_1 p_a p_b \delta\nu^2$ principally acts on the distance between the different curves. Numerical simulations have shown that with realistic rf field strengths (between 0.8 and 2.3 kHz), reasonable precision on the signal intensities (10% of the intensity at $\theta_S = 0°$) and in the case of $\delta\nu$ on the order of 100 Hz, determination of exchange correlation times between about 90 μs and 400 μs should be feasible. This range depends strongly on these three parameters.

Table 1. Effect of the angle θ_I of the effective field experienced by the proton on the T_1/T_2 ratio and A coefficient determined by fitting the simulated curve $\langle S_Z^{eq} \rangle = f(\theta_S, \omega_1^S)$ with Equation 5

θ_I	Ile 35			Thr 21		
	A	T_1/T_2	%	A	T_1/T_2	%
0°	1.279	1.923	11.1	1.204	1.953	9.7
10°	0.972	1.918	11.4	0.915	1.956	9.6
20°	0.873	1.925	11.1	0.829	1.970	8.9
30°	0.817	1.954	9.7	0.787	1.998	7.6
40°	0.778	2.000	7.6	0.758	2.038	5.8
50°	0.751	2.051	5.2	0.738	2.078	3.9
60°	0.732	2.097	3.1	0.723	2.112	2.4
70°	0.720	2.132	1.5	0.714	2.142	1.0
80°	0.713	2.157	0.3	0.709	2.158	0.2
90°	0.710	2.164	0.0	0.707	2.163	0.0

The two amino acids have a different surrounding proton density. 34 and 26 protons are found in a 6 Å sphere around Ile 35 and Thr 21 nitrogens, respectively. The columns labeled % contain the deviation of the T_1/T_2 ratio relatively to the exact value obtained for $\theta_I = 90°$.

Pulse sequence

The measurement of ^{15}N steady-state magnetization in the presence of off-resonance rf irradiation was performed using the pulse sequence shown in Figure 2A. The sequence starts with irradiation on the ^{15}N channel in order to reach the steady state. Then a 90° hard pulse, followed by the evolution delay t_1, is applied to allow frequency labeling in the indirect dimension. Finally an inverse INEPT transfer with sensitivity enhancement (Cavanagh et al., 1991) and pulsed field gradients for the coherence selection (Kay et al., 1992) is used to detect the signal on the proton channel.

The irradiation part includes different features in order to let the ^{15}N magnetization reach values close to the steady state in the shortest irradiation time τ_m. Firstly the protons are spin-locked before the nitrogens. Proton irradiation requires less power level than for nitrogen and is thus less demanding on the experimental apparatus. In this way, the proton magnetization is better saturated and the ^{15}N magnetization has already started to relax towards its final value

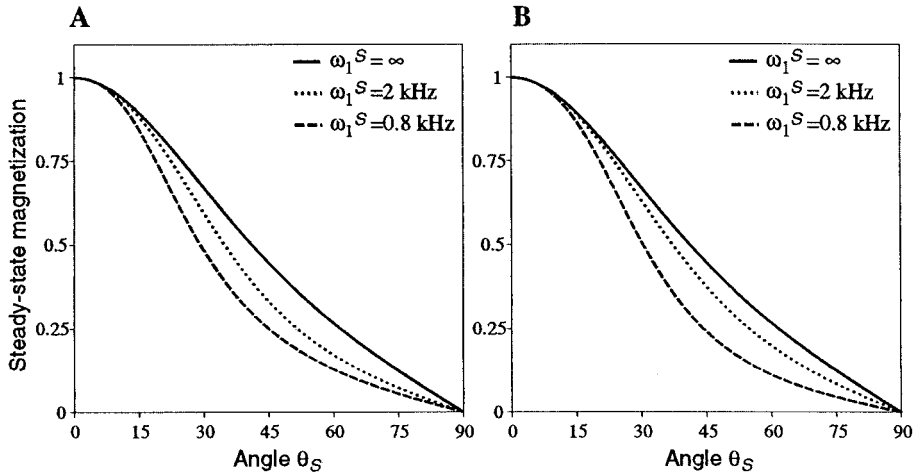

Figure 1. Numerical simulation of the ^{15}N steady-state magnetization as a function of the rf field strength and of the angle θ_S with fast exchange contribution to relaxation. The parameters for these simulations are: $T_1 = 0.414$ s, $T_1/T_2 = 2.163$, $\delta\nu = 100$ Hz. (A) $\tau_e = 80$ μs. (B) $\tau_e = 200$ μs.

because heteronuclear dipolar cross-relaxation is canceled. The proton irradiation is composed of a 90° hard pulse applied in the amide frequency domain followed by a WALTZ 16 decoupling scheme. We thus benefit from the WALTZ 16 effective field and obtain the condition $\theta_I > 70°$ with a lower power requirement.

Irradiation on the nitrogen spins is switched on abruptly at the chosen amplitude and offset, but is switched off at the end of the spin-lock via a linear ramp to enable an adiabatic rotation of the nitrogen magnetization towards the static magnetic field (Desvaux et al., 1995a). This feature is not used at the beginning of the irradiation, since the induced projection ($\cos\theta_S$ factor) leads to initial conditions closer to the desired steady-state value, so that a shorter irradiation duration is needed. In this procedure we also profit from the increase of $1/T_{1\rho}^{\text{off}}$ with θ_S, so that for high θ_S values, where the value resulting from the projection ($\cos\theta_S$) is very different from the final result (Equation 5 or 8), the relaxation is much faster than $1/T_1$. Using numerical simulations, we have observed that for $1/T_1 = 2.5$ Hz and $I/T_2 = 5.5$ Hz and for a recovery delay $T = 1.5$ s, the steady-state value is reached at a level better than 2% whatever θ_S, as long as τ_m is greater than about 850 ms. We have consequently used τ_m values of this order of magnitude.

Finally, the recovery delay T could theoretically be optimized since the steady-state magnetization is less than the equilibrium value. We actually could not benefit from this feature, since a high repetition rate would increase the amplifiers duty cycle (total energy delivered by time unit), which is already the main hardware constraint.

For the acquisition of the 2D map at $\theta_S = 0°$, temperature fluctuations resulting from different irradiation durations (Wang and Bax, 1993) were controlled by changing the beginning of the pulse sequence as follows (Figure 2B). An off-resonance rf irradiation of the same duration τ_m is applied during the recovery delay T, while no irradiation is applied during τ_m. In this sequence, adiabatic rotations are used at the two ends of the irradiation to avoid magnetization losses due to projection along the effective field (Desvaux et al., 1995a), and the angle θ_S is chosen as small as possible (with an offset still compatible with proper tuning of the probe). The value at $\theta_S = 0°$ can then safely be compared to the steady-state values at larger θ_S.

First experiments: Evidence of biases

The classical procedure to measure heteronuclear transverse or off-resonance self-relaxation rates is based on transient measurements (Kay et al., 1989; Peng and Wagner, 1992; Zinn-Justin et al., 1997). The sequence is composed of an INEPT transfer followed by an irradiation of duration τ'_m during which the magnetization relaxes. In the same way as for the steady-state measurement, the magnetization is then labeled in frequency by a transverse evolution during t_1 and back-transfered to proton by an inverse INEPT for detection. In this scheme, for long mixing times τ'_m, the signal is on the same order of magnitude as the

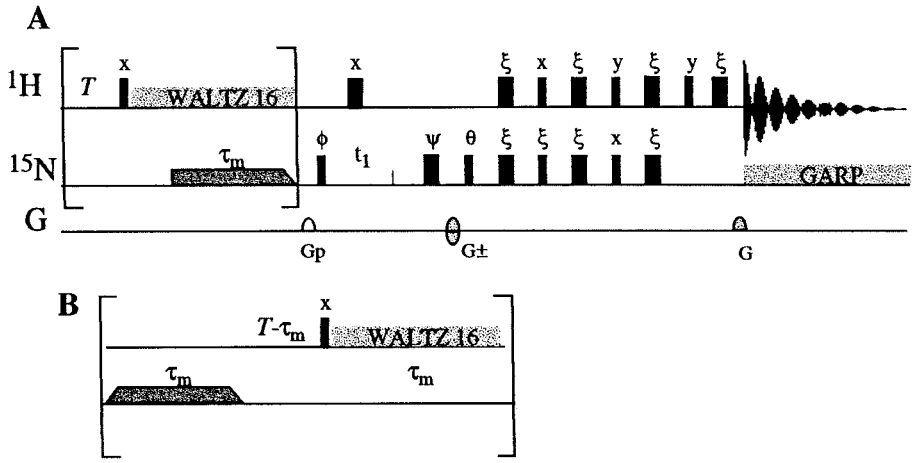

Figure 2. (A) Pulse sequence used to measure the ^{15}N steady-state magnetization in the presence of off-resonance rf irradiation ($\theta_S > 0$). The upper line shows the proton channel, the middle line the nitrogen-15 channel and the bottom line the pulsed field gradient. Thin vertical bars represent 90° pulses, thick vertical bars 180° pulses and shaded symbols represent shaped pulses or composite multipulse sequences. Gp is a purging gradient pulse while G± and G are encoding gradient pulses. The phase cycle is ϕ = x,−x, ξ = y,y,−y,−y, ψ = x,x,−x,−x. The receiver phase cycle is x, −x, −x, x. The States-TPPI mode is achieved firstly by changing θ from y to −y and changing the sign of the first encoding gradient pulse every FID, and secondly by inverting ϕ and the receiver phase every two FIDs (Kay et al., 1992). The proton spin-lock is obtained by a WALTZ16 composite pulse sequence, while the nitrogen off-resonance rf irradiation is shaped for adiabatic rotation only at the end. Nitrogen decoupling is achieved by a GARP sequence. For $\theta_S = 0°$ the part in brackets in the sequence is replaced by the scheme depicted in B. The nitrogen off-resonance rf irradiation is now shaped for adiabatic rotations at both ends.

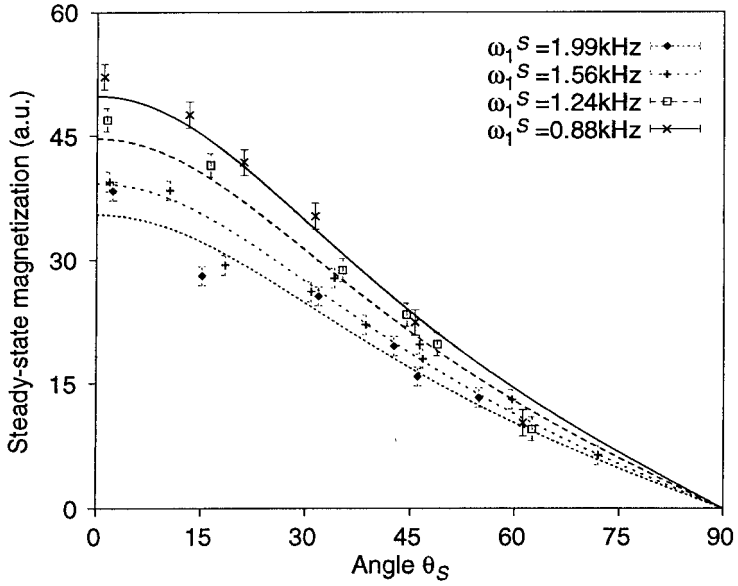

Figure 3. ^{15}N steady-state magnetization of Val-27 in the presence of a nitrogen off-resonance rf irradiation of strength ω_1^S. The spectra were acquired at 14 T using one X amplifier. Using one T_1/T_2 value and four different A values (Equation 5), each one associated to one of the four ω_1^S values, the best-fit T_1/T_2 value is equal to 1.95 ± 0.10.

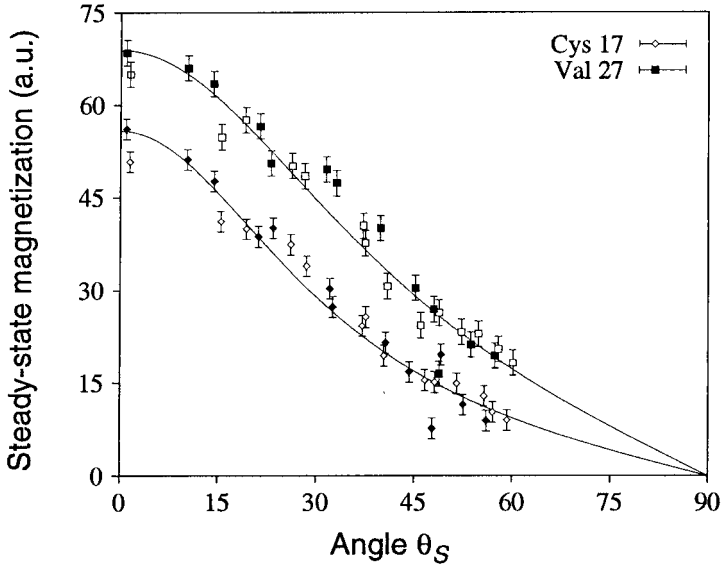

Figure 4. ^{15}N steady-state magnetization of Cys 17 and Val 27 (signal intensities multiplied by 1.5 for clarity reasons) in the presence of an off-resonance rf irradiation on the nitrogen. The experiments were acquired at 11.7 T using two X broadband amplifiers. Two different rf field strengths, 0.9 kHz (filled symbols) and 1.4 kHz (open symbols), were used. The limit value A is independent of the rf field strength. The best-fit T_1/T_2 ratios are 3.68±0.18 and 2.34±0.12 for Cys 17 and Val 27, respectively. The fast exchange contribution to relaxation on Cys 17 leads to an increase of the T_1/T_2 ratio.

steady-state magnetization. This example illustrates the similarity between the transient and steady-state approaches. In view of the widespread confidence in the determination of self-relaxation rates by the transient approach, we hoped for good accuracy in the steady-state method. However, despite these similarities, the results obtained at the first stage of this study show how biases are present and may prevent a direct use of the steady-state method.

Figure 3 shows the variation of the steady-state magnetization as a function of the angle θ_S for different rf field strengths obtained at 14 T with a 5 mm ^{1}H/^{13}C/^{15}N probehead. The amplifier is a Bruker BLAXH-300. Although the curves correctly fit the data points with the same T_1/T_2, the initial signal amplitudes A decrease with the rf field strength ω_1^S, in complete contradiction with the theory. This observation is actually a consequence of the rf irradiation which induced a measurable power drop of the amplifier at full power, making the following hard pulses miscalibrated (See Guenneugues et al. (1999a) for a more detailed discussion of this phenomenon).

Using different A for each rf field strengths, that is increasing the number of adjusted parameters, is obviously not suitable to achieve a very high precision and to allow fine characterization of fast exchange processes.

Correction of the instrumental biases

To circumvent this problem, we first used two X-amplifiers, a Bruker BLAX-300 for the rf irradiation and a Bruker BLAXH-300 for the hard pulses and decoupling. The amplifier outputs were coupled before the preamplifier, a scheme requiring fine tuning of the probehead. The BB-I probehead equipped with z gradient provided the best results in terms of hard pulse length following strong rf irradiation. Figure 4 displays results obtained with this setup (see figure caption). There is no differential scaling between the curves at different rf field strengths, showing that the amplifiers do not suffer a power drop any more. However, a relatively large distribution of the points around the best fit theoretical curve is still observed, not correlated with the rf field strength, which renders difficult the discrimination between the behaviors described by Equations 5 and 8. This is illustrated by amide Cys 17. A much larger T_1/T_2 value than for Val 27 is observed, indicative of the presence of an exchange contribution, but no systematic deviation between the steady-state signal intensities acquired with the two different rf fields can be evidenced.

In addition, suspecting that the presence of biases might lead to non-Gaussian normal noise, when requesting a large power from the electronics, we have performed a number of statistical tests. A series of

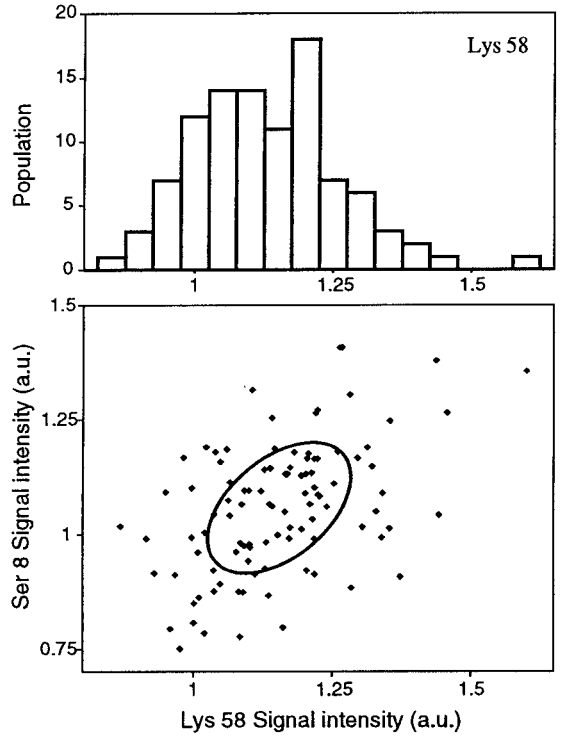

Figure 5. Example of the experimental statistical distribution of the ^{15}N steady-state magnetization. Top: the distribution of intensities for Lys 58. The first and third moments of the distribution almost vanish, and the ratio of the square of the second to fourth moment ($M_2{}^2/M_4$) is equal to 0.28, while for a Gaussian distribution it is found to be equal to 1/3. For Ser 8, the same ratio is equal to 0.35. Bottom: signal intensities of two isolated peaks (Lys 58 and Ser 8) in the 1D spectrum are represented for each of the 100 different spectra (700 ms irradiation at 1.36 kHz and 25°, use of two X amplifiers). The ellipse corresponds to the distribution at one standard deviation, showing a correlation between the fluctuations of the intensities of the two amide nitrogens. The correlation coefficient r^2 between the signal intensities of Ser 8 and Lys 58 is equal to 0.47. Similar results are obtained for other residues and other experimental conditions (different τ_m, θ_S and ω_1^S values).

100 FIDs was acquired for a given value of θ_S and ω_1^S. This series was repeated for different angles θ_S and different rf field strengths ω_1^S. For each (θ_S, ω_1^S) pair, isolated peaks were integrated and the sets of intensities were used for statistical analysis by computing their average values, their distributions and their standard deviations. The different moments of the distribution indicate that the noise remains Gaussian. However, the correlation of the fluctuations of two different peak intensities deduced from the off-diagonal terms of the correlation matrices or from a linear regression analysis is not null. As an example, Figure 5 shows the results for Lys 58, and for Lys 58 against Ser 8. From their analyses we deduce that about half the fluctuations of the intensities around the average value do not result from random noise but originate from experimental biases limiting the attainable precision of the measurements. This correlation increases for large ω_1^S values, further confirming the presence of instrumental artifacts.

Reliable determinations of the T_1/T_2 ratios

The availability of an X-amplifier (500 W) of a new generation, kindly lent to us by the Bruker company, allowed us to switch back to the initial scheme, that is, to use the same amplifier for all ^{15}N pulses under conditions far from the limits of its capacities. Figure 6 displays the experimental variation of the steady-state value as a function of the angle θ_S obtained with this setup on a 11.7 T spectrometer with a BB-I one axis gradient probehead. Two different rf field strengths of 840 Hz and 1730 Hz, respectively, were employed with 11 angles θ_S for each, this set is called **A** in the following. A further reduction in the dispersion of experimental points from the best fit theoretical curve is observed relative to that observed using two X amplifiers (Figure 4). From this dataset **A** of steady-state signal intensities, the T_1/T_2 ratios were refined considering the effect of the B_1 field homogeneity. For each voxel of the sample characterized by an rf field B_1 (v), the steady-state signal intensity of this voxel is given by Equation 5. The acquired signal intensity is obtained by a weighted summation of the steady-state signal intensity for each B_1 field value. This weight is given by the experimentally determined distribution of the B_1 field inside the sample (Guenneugues et al., 1999a). We have checked by randomly modifying the distribution that the T_1/T_2 values are very weakly affected. With a Gaussian noise of 10% of the maximum signal intensity applied on each point, the average T_1/T_2 value varies by less than 0.9%. We have also considered the effect of the digitization of the B_1 distribution by varying the processing parameters (apodization functions, zero-filling, ...). It leads to a variation of the average T_1/T_2 value inferior to 0.1%. However, we have noticed that the Flatt algorithm for baseline correction may induce larger variation at the opposite of polynomial correction.

Figure 7 shows the comparison of the T_1/T_2 ratios obtained by the steady-state measurement (with correction for the rf field inhomogeneity) with those derived from separate self-relaxation times measurements (determined from the fitting of 11 decay curves corresponding to longitudinal, transverse and off-resonance self-relaxation rates (Guenneugues et al.,

1997)). For the comparison of these values, we consider only residues whose chemical exchange contribution to relaxation, if any, does not affect the T_1/T_2 value obtained with the considered effective field ($\Omega_S > 1$ kHz). We first consider the sets obtained by the transient method and by the steady-state method without correction for the rf field inhomogeneity (not shown in the figure). The T_1/T_2 ratio obtained by the steady-state method is underestimated by 5.2% relative to the values obtained by the transient method. By contrast, the two data sets obtained by the transient method and the steady-state measurement with correction for the rf field inhomogeneity are indistinguishable. The average pairwise difference between the T_1/T_2 values is less than 0.004, with a standard deviation of 0.18. Based on T-tests at a 95% level of confidence, for each residue except Glu 37, Gly 41 and Cys 53 (no residue at 99.2% confidence level), the T_1/T_2 ratios obtained by the transient and steady-state method are indistinguishable. This good agreement validates the steady-state magnetization measurement as a method for T_1/T_2 determination. The nuclei undergoing fast exchange processes can then be identified by their T_1/T_2 values significantly higher than the average. This is the case, for instance, for Cys 17, Glu 20 or Thr 21.

Attempts to characterize fast exchange

To explore the possibility of determining fast exchange correlation times, we have analyzed two sets of data points: the one corresponding to Figures 6 and 7 (dataset **A**) and another set (dataset **B**) acquired separately ($\gamma_N B_1 = 1460$ Hz, 16 angles θ_S). The scattering of points around the best-fit theoretical curve and the relatively small fast exchange contribution to relaxation as determined in a previous study (Zinn-Justin et al., 1997) prevent any confidence in a direct fit of the data. As an alternative, we have attempted to use the following procedure. Taking into account the complete sets (**A** + **B**) of steady-state signal intensities corresponding to each ^{15}N nucleus and their associated uncertainties, we have built 500 synthetic data sets as described in the section Materials and methods. Each of these sets was fitted against Equation 8. To accept or reject the fit, we applied criteria of selection based on the χ^2 value and on the physical relevance of the different parameters (T_1/T_2 value around the protein average value, τ_e compatible with the explored range of effective field amplitudes and a reasonable $T_1 p_a p_b \delta\nu^2$ value). We can then define a success rate by computing the ratio of accepted fits over the number of attempts. This procedure allows us also to define a range of exchange correlation time which is compatible with the experimental measurements. Although these correlation times cannot be determined with high confidence, tendencies in agreement with what was previously reported for toxin α (Zinn Justin et al., 1997) could be observed. Nevertheless, the success rate was always low, since the highest obtained value was 14% for Ile 35, and the apparent qualitative agreement cannot be considered as conclusive.

Discussion

The measurement of the steady-state magnetization of the heteronucleus as a function of the angle θ_S and of the rf field amplitude ω_1^S could represent an alternative to the classical transient method for the determination of the heteronucleus T_1/T_2 ratio and the detection of fast exchange with characteristic times around 100 μs. From a theoretical point of view, this method seems promising, since:

1. The parameters are deduced from a least-squares fitting procedure based on an analytical equation valid for any motion and any relaxation mechanism.
2. Experimental biases such as rf field inhomogeneity can be accounted for.
3. Information on dynamics is directly related to the signal intensity.

Experimentally, the sensitivity of this approach to hardware biases, particularly the amplifier power drops, has made its practical validation difficult.

On toxin α, using a 500W X-amplifier and a BB-I probehead, we have however succeeded in obtaining apparently bias-free measurements and T_1/T_2 ratios in agreement with those derived from self-relaxation rate determinations. The accuracy of the determination of the T_1/T_2 ratios determined from the set **A** is found equal to slightly less than 5%, as deduced from Monte Carlo simulation. This figure represents already an improvement over the T_1/T_2 ratio deduced from transient experiments (Guenneugues et al., 1997), where the longitudinal and transverse self-relaxation rates were determined by fitting to Equation 2 a set of data composed of a longitudinal, a transverse and 9 off-resonance self-relaxation rates (Zinn-Justin et al., 1997). With an average reduced χ^2 of about 1 for this fitting procedure, we reported a precision of about 4 to 5% for the separate determination of T_1 and T_2, lead-

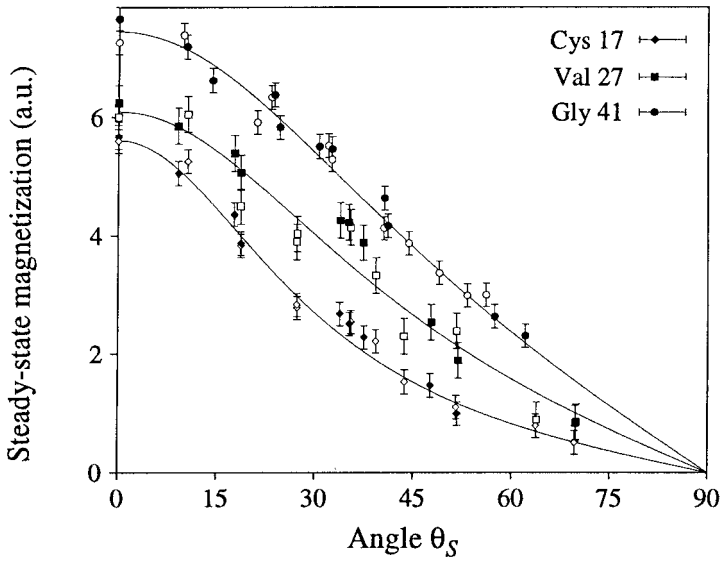

Figure 6. Experimental variation of the ^{15}N steady-state magnetization as a function of the rf field intensity and the angle θ_S between the static and the effective fields in the rotating frame for Gly 41, Val 27 (signal intensities multiplied by 1.5 for clarity reasons) and Cys 17 at two rf field strengths $\omega_1^S = 840$ Hz (filled symbols) and 1730 Hz (open symbols). The best-fit T_1/T_2 values are 1.76±0.06, 2.24±0.15 and 4.20±0.23, respectively. For the latter, even if a contribution from fast exchange should be present because of the large T_1/T_2 ratio, the range of effective fields explored does not allow the characterization of the exchange correlation time. Indeed, no significant difference between the steady-state magnetization corresponding to the two rf fields used is detectable. The exchange correlation time is then expected to be shorter than about 80 μs.

ing to an uncertainty of 7.1% on their ratio. Of course all these values appear largely higher than the 1% precision reported on the T_1 or T_2 measurements based on reproducibility experiments. However, a reproducibility at a 1% level does not mean 1% of uncertainty. This is substantiated by the statistical analysis of these high precision measurements for which χ^2 tests have shown large discrepancies which could be interpreted as an underestimation of the 1% level of error by a factor between 4 and 5 (Lee et al., 1997). The presence of larger uncertainties than what reproducibility experiments measure can result from systematic biases, which had in fact been shown to be present (Guenneugues et al., 1999a). On the other hand, since for our transient measurements the T_1 and T_2 values were derived from the least-squares fitting to Equation 2 of 11 independent measurements, it seems reasonable thinking that the resulting uncertainties on T_1 and T_2 take into account the biases present in each separate decay curve.

Pushing further the comparison between the steady-state and the transient approaches requires the comparison of their relative sensitivities. On the one hand, the steady-state magnetization method suffers from using the thermal polarization of ^{15}N and not

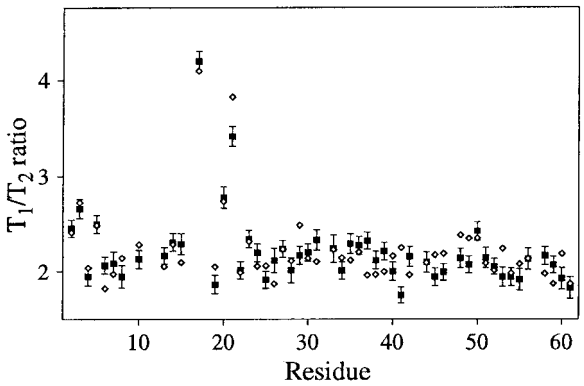

Figure 7. Comparison of the T_1/T_2 ratio obtained using steady-state magnetization measurement taking into account the B_1 inhomogeneity (filled symbol with error bars) and relaxation decay curves (open symbol). For the sake of clarity the error bars of the latter were not added, they are about 1.5 times as large as those of the steady-state measurements.

from that of protons. However, it would be too far reaching to conclude, based on this remark, that the transient method has a much higher sensitivity, despite the need of recording a larger number of 2D spectra to determine the relaxation rates. Indeed, in the transient experiments the magnetization relaxes during the mixing time τ'_m, decreasing the sensitivity for the sig-

nals acquired with the longest mixing time. It becomes consequently difficult to perform a precise comparison since the choice of the mixing times influences the sensitivity. If, as an example, we consider the optimum sampling strategy (Jones, 1997), then 4 out of the 5 points have to be acquired at a mixing time τ'_m of 1.3 T with T the self-relaxation time. For this mixing time value, the signal has decreased to 0.27 times its initial intensity. The gain in sensitivity resulting from the polarization transfer from the proton is very reduced, and can become negligible, if the efficiency of the $^1H \rightarrow ^{15}N$ INEPT transfer is not maximal. On the other hand, the transient experiments are sensible to electronic biases (Guenneugues et al., 1999a), such as the amplifier power drop observed in the present study. Detecting a non-exponential behavior resulting, for instance, from the rf field inhomogeneity is impossible with the use of the optimal sampling strategy, and more than 5 points in the decay curve are then needed (Jones, 1997). As a consequence, it seems difficult at the present time to formally conclude which approach should give the most accurate T_1/T_2 ratio in the shortest experiment time. It is, indeed, expected to strongly depend on the studied system (heteronucleus, T_2 value, quality of the electronics, ...). We determine the T_1/T_2 ratios represented in Figure 7 based on the dataset **A** with an experiment time of about 4.5 days and obtain a precision of about 5%. This duration would allow the separate determination of the longitudinal and transverse self-relaxation with a very high precision. If the only interest lies in the T_1/T_2 ratios, the experiment time of the steady-state method can certainly be shortened by using only one rf field strength. This is confirmed by studying the dataset **B**, obtained in a shorter experiment time. The precision on the T_1/T_2 determination is on the order of 6%, with an average reduced χ^2 value of about 1. Moreover the T_1/T_2 ratios are in complete agreement with the values presented in Figure 7, even if the two measurements **A** and **B** are totally independent. A priori using only one rf field strength with a limited value (say around 1.2 kHz) would allow a reduction of the experiment time by enabling a faster repetition rate, while non-linearity of the electronic response could still he avoided. The method is even very powerful to extract a crude estimate of the average T_1/T_2 ratio over all the residues in order to derive the overall correlation time of the protein in different conditions. This is the case, for instance, when oligomerisation is suspected to occur and one wants to check different pHs, temperatures or protein concentrations (Fushman et al., 1997). With 3 points acquired at angle values close to 0, 40 and 50°, one can obtain T_1/T_2 ratios with large uncertainties on a per residue basis but still providing the correct average. Using the subset from dataset **B** composed of the points acquired with angles of 5, 44 and 48°, we find an average T_1/T_2 ratio of 2.24 ± 0.4 against 2.19 ± 0.4 with the transient method. Various experimental conditions can thus be scanned in less than a day.

The second goal of the present investigation concerned the characterization of fast exchange. With the protein used and the present uncertainty, this turns out to be impossible. First, from the previous study based on transient measurements (Zinn-Justin et al., 1997), it appears that no nitrogen amide of toxin α does experience an exchange with a large chemical shift difference $\delta\nu$ between the two conformations (the largest value reported was about 2 ppm for Thr-21). Second, the instability of the rf amplifier resulting from the quality of the probehead prevented increasing this exchange contribution by increasing the static magnetic field. Moreover, electronics constraints made it impossible to use a very large rf field amplitude (here $\omega_1^S < 1.75$ kHz), which limits the range of the effective field Ω_S. This puts at a disadvantage the analysis of the largest chemical exchange contributions corresponding to Cys 17, Glu 20 and Thr 21 amide nitrogen, because their exchange correlation times are typically shorter than 80 μs. Indeed, at the opposite to the successful determination of exchange correlation time by the transient method (Zinn-Justin et al., 1997), which simultaneously used CPMG and off-resonance rates to sample a larger range of effective fields (Desvaux and Berthault, 1999; Mulder et al., 1999) in the present study, we were closer to the range of effective fields accessible using only off-resonance self-relaxation rates measurements as in the method described by Akke and Palmer (1996). The points corresponding to the lowest effective field amplitudes are those with the largest angles θ_S and are consequently those with the smallest sensitivity. The major consequence of this is to reduce the range of exchange correlation times which can be determined. Combining the steady state magnetization method with the T_2 values extracted from a CPMG sequence would probably help the characterization of exchange.

At the end of this experimental study, the initial hopes, which were to increase the accuracy in the determination of the T_1/T_2 ratios and of the exchange correlation times, are barely reached. We believe that with the present available electronics, it is almost

impossible to obtain better characterization of the exchange on this sample of toxin α in a 11.7 T static magnetic field by the steady-state method. Our two principal limits with this sample were the relatively long T_2, which implies long irradiations, and thus large load on the amplifiers, and the small exchange contribution.

To perform confident measurements with the steady-state method, it seems essential to avoid working at the limits of the electronics. This, in particular, means that the energy of irradiation needed to reach the steady state should be minimized. The different options to fulfill these conditions are (i) working with very high power amplifiers and with probeheads with a high quality factor (excellent sensitivity) in order to avoid needing a too large power for obtaining large rf field amplitudes; (ii) decreasing the irradiation duration by using proteins with a shorter self-relaxation time, for instance paramagnetic proteins for which fast exchange has been reported (Banci et al., 1998) or (iii) dealing with other heteronuclei such as ^{13}C or ^{31}P for which the larger gyromagnetic ratio might enable one to decrease the power requirement and obtain a better sensitivity. These last two points are also those where the sensitivity would be more in favor of the steady-state approach.

Acknowledgements

We are grateful to Dr. Martial Piotto from Bruker France for providing us with a BLAX-500 amplifier and high power couplers. Marc Guenneugues acknowledges IFSBM (Villejuif) for a grant support.

References

Akke, M. and Palmer III, A.G. (1996) *J. Am. Chem. Soc.*, **118**, 911–912.

Akke, M., Liu, J., Cavanagh, J., Erickson, H.P. and Palmer III, A.G. (1998) *Nat. Struct. Biol.*, **5**, 55–59.

Banci, L., Bertini, I., Cavazza, C., Felli, I.C. and Koulougliotis, D. (1998) *Biochemistry*, **37**, 12320–12330.

Brüschweiler, R. and Ernst, R.R. (1992) *J. Chem. Phys.*, **96**, 1758–1766.

Brüschweiler, R., Liao, X. and Wright, P. (1995) *Science*, **268**, 886–889.

Cavanagh, J., Palmer III, A.G, Wright, P.E. and Rance, M. (1991) *J. Magn. Reson.*, **91**, 429–436.

Davis, D.G., Perlman, M.E. and London, R.E. (1994) *J. Magn. Reson.*, **B104**, 266–275.

de Alba, E., Baber, J.L. and Tjandra, N. (1999) *J. Am. Chem. Soc.*, **121**, 4282–4283.

Desvaux, H. and Goldman, M. (1992) *Mol. Phys.*, **81**, 955–975.

Desvaux, H., Berthault, P., Birlirakis, N., Goldman, M. and Piotto, M. (1995a) *J. Magn. Reson.*, **A113**, 47–52.

Desvaux, H.J., Birlirakis, N., Wary, C. and Berthault, P. (1995b) *Mol. Phys.*, **86**, 1059–1073.

Desvaux, H. and Berthault, P. (1999) *Prog. NMR Spectrosc.*, **35**, 295–340.

Deverell, C., Morgan, R.E. and Stange, J.H. (1970) *Mol. Phys.*, **18**, 553–559.

Drevet, P., Lemaire, C., Gasparini, S., Zinn-Justin, S., Lajeunesse, E., Ducancel, F., Trémeau, O., Courson, M., Boulain, J.-C. and Ménez, A. (1997) *Protein Express. Purif.*, **10**, 293–300.

FELIX Manual (1995) Biosym/MSI, San Diego, CA.

Felli, I.C., Desvaux, H. and Bodenhausen, G. (1998) *J. Biomol. NMR*, **12**, 209–521.

Fushman, D., Cahill, S. and Cowburn, D. (1997) *J. Mol. Biol.*, **266**, 173–194.

Fushman, D., Tjandra, N. and Cowburn, D. (1998) *J. Am. Chem. Soc.*, **120**, 10947–10952.

Goldman, M. (1999) *Adv. Magn. Opt. Reson.*, In press.

Guenneugues, M., Drevet, P., Pinkasfeld, S., Gilquin, B., Ménez, A. and Zinn-Justin, S. (1997) *Biochemistry*, **36**, 16097–16108.

Guenneugues, M., Berthault, P. and Desvaux, H. (1999a) *J. Magn. Reson.*, **136**, 118–126.

Guenneugues, M., Gilquin, B., Wolff, N., Ménez, A. and Zinn-Justin, S. (1999b) *J. Biomol. NMR*, **14**, 47–66.

Jones, J.A. (1997) *J. Magn. Reson.*, **126**, 283–286.

Kay, L.E., Torchia, D.A. and Bax, A. (1989) *Biochemistry*, **28**, 8972–8979.

Kay, L.E., Keifer, P. and Saarinen, T. (1992) *J. Am. Chem. Soc.*, **114**, 10663–10665.

Kroenke, C.D., Loria, J.P., Lee, L.K., Rance, M. and Palmer III, A.G. (1998) *J. Am. Chem. Soc.*, **120**, 7905–7915.

Lee, L.K., Rance, M., Chazin, W.J. and Palmer III, A.G. (1997) *J. Biomol. NMR*, **9**, 287–298.

Mandel, A.M. and Palmer III, A.G. (1994) *J. Magn. Reson.*, **A110**, 62–72.

Mulder, F.A., van Tilborg, P.J., Kaptein, R. and Boelens, R. (1999) *J. Biomol. NMR*, **13**, 275–288.

Orekhov, V.Y., Pervushin, K.V. and Arseniev, A.S. (1994) *Eur. J. Biochem.*, **219**, 887–896.

Palmer III, A.G., Williams, J. and McDermott, A. (1996) *J. Phys. Chem.*, **100**, 13293–13310.

Peng, J.W. and Wagner, G. (1992) *J. Magn. Reson.*, **98**, 308–332.

Press, W.H., Flannery, B.P., Teukolsky, S.A. and Vetterling, W.T. (1992) *Numerical Recipes in C*, 2nd edition, Cambridge University Press, Cambridge

Szyperski, T., Luginbühl, P., Otting, G., Güntert, P. and Wüthrich, K. (1993) *J. Biomol. NMR*, **3**, 151–164.

Tjandra, N., Feller, S.E., Pastor, R.W. and Bax, A. (1995) *J. Am. Chem. Soc.*, **117**, 12562–12566.

Tjandra, N., Szabo, A. and Bax, A. (1996a) *J. Am. Chem. Soc.*, **118**, 6986–6991.

Tjandra, N., Wingfield, P., Stahl, S. and Bax, A. (1996b) *J. Biomol. NMR*, **8**, 273–284.

Wagner, G. (1993) *Curr. Opin. Struct. Biol.*, **3**, 748–754.

Wang, A.C. and Bax, A. (1993) *J. Biomol. NMR*, **3**, 715–720.

Zinn-Justin, S., Roumestand, C., Gilquin, B., Bontems, F., Ménez, A. and Toma, F. (1992) *Biochemistry*, **31**, 11335–11347.

Zinn-Justin, S., Berthault, P., Guenneugues, M. and Desvaux, H. (1997) *J. Biomol. NMR*, **10**, 363–372.